

Supporting Information

Tuning the Distance of Rattle-Shaped IONP@Shell-in-Shell Nanoparticles for Magnetically-Targeted Photothermal Therapy in the Second Near-Infrared Window

Ming-Fong Tsai¹, Chin Hsu², Chen-Sheng Yeh³, Yu-Jen Hsiao⁴, Chia-Hao Su^{5,6*} and Li-Fang Wang^{1,7,8*}

¹Department of Medicinal and Applied Chemistry, College of Life Sciences, Kaohsiung Medical University, Kaohsiung 807, Taiwan

²Department of Physiology, Faculty of Medicine, College of Medicine, Kaohsiung Medical University, Kaohsiung 807, Taiwan

³Department of Chemistry, Center for Micro/Nano Science and Technology, and Advanced Optoelectronic Technology Center, National Cheng Kung University, Tainan 701, Taiwan

⁴National Nano Device Laboratories, National Applied Research Laboratories, Tainan 701, Taiwan

⁵Institute for Translational Research in Biomedicine, Kaohsiung Chang Gung Memorial Hospital, Kaohsiung 833, Taiwan

⁶Department of Biomedical Imaging and Radiological Sciences, National Yang Ming University, Taipei 112, Taiwan

⁷Department of Medical Research, Kaohsiung Medical University Hospital, Kaohsiung 807, Taiwan

⁸Institute of Medical Science and Technology, National Sun Yat-Sen University, Kaohsiung 804, Taiwan

*Corresponding authors

Correspondence to: Li-Fang Wang, E-mail: lfwang@kmu.edu.tw

Chia-Hao Su, E-mail: chiralsu@adm.cgmh.org.tw

Table S1. Sizes and thicknesses of IONP@shell-in-shell at various amounts of H_{AuCl}₄ in feed

H_{AuCl}₄	Diameter	External Shell thickness	Shell gap
1.0 μmole	66.7 nm± 4.8 nm	6.7 nm± 0.8 nm	9.6 nm± 1.9 nm
1.5 μmole	68.2 nm± 4.6 nm	8.1 nm± 0.6 nm	6.5 nm± 1.2 nm
2.0 μmole	70.1 nm± 5.1 nm	9.4 nm± 0.7 nm	4.3 nm± 0.8 nm

Estimated from TEM images

Table S2. Fe/Ag/Au compositions of IONP@shell-in-shell at various amounts of H_{AuCl}₄ in feed

H_{AuCl}₄	Fe %	Ag %	Au %
1.0 μmole	17.6%	53.7%	28.7%
1.5 μmole	17.1%	46.4%	36.5%
2.0 μmole	16.4%	41.6%	42.0%

Analyzed by inductively coupled plasma-atomic emission spectrometry

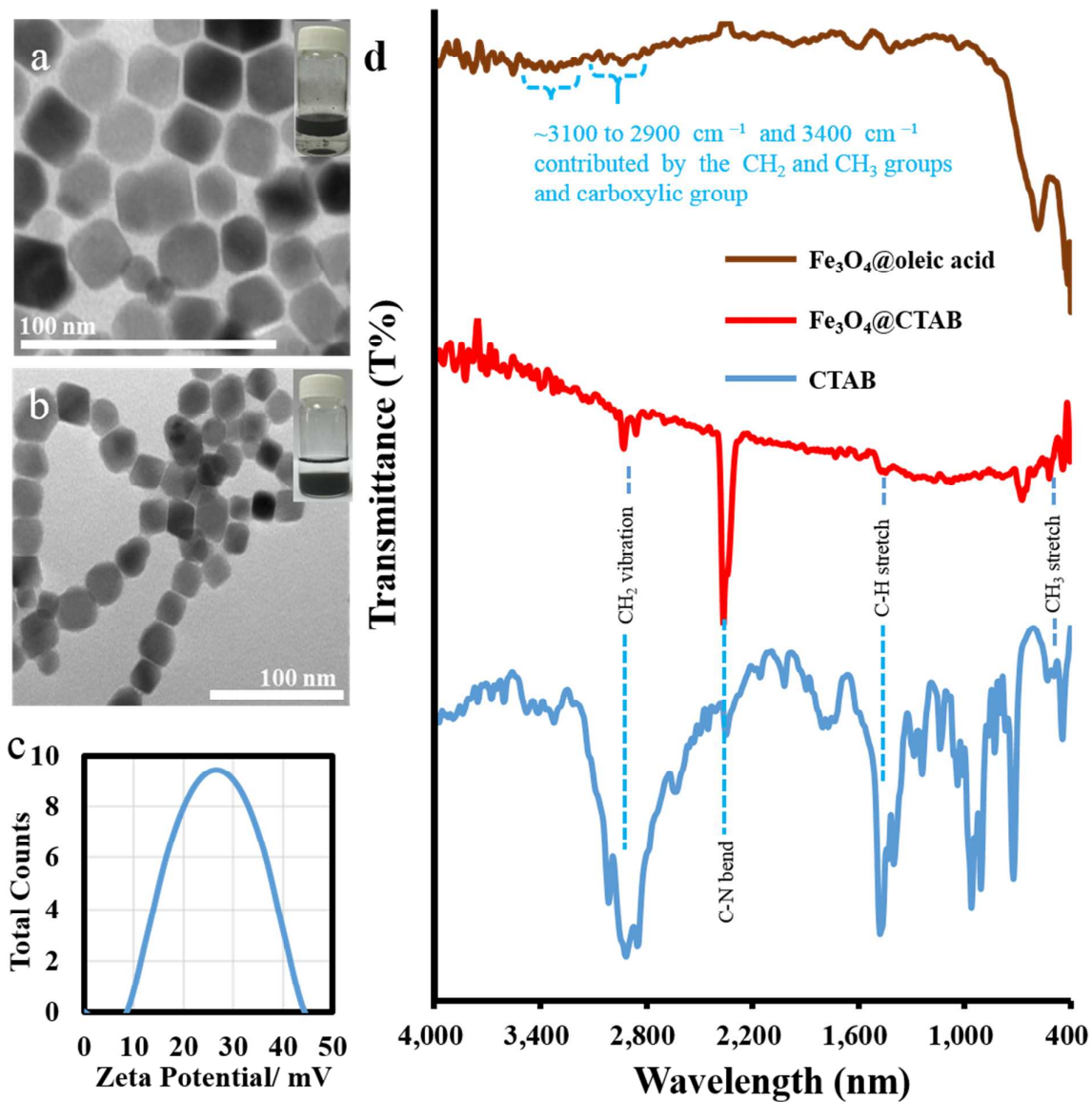


Figure S1. TEM images of (a) hydrophobic $\text{Fe}_3\text{O}_4@$ oleic acid NPs; insets: $\text{Fe}_3\text{O}_4@$ oleic acid NPs dispersed in hexane and (b) hydrophilic $\text{Fe}_3\text{O}_4@$ CTAB NPs (IONPs); insets: IONPs dispersed in DD water. (c) Zeta potential of IONPs and (d) FTIR spectra of $\text{Fe}_3\text{O}_4@$ oleic acid NPs (brown), $\text{Fe}_3\text{O}_4@$ CTAB NPs (red) and CTAB (blue).

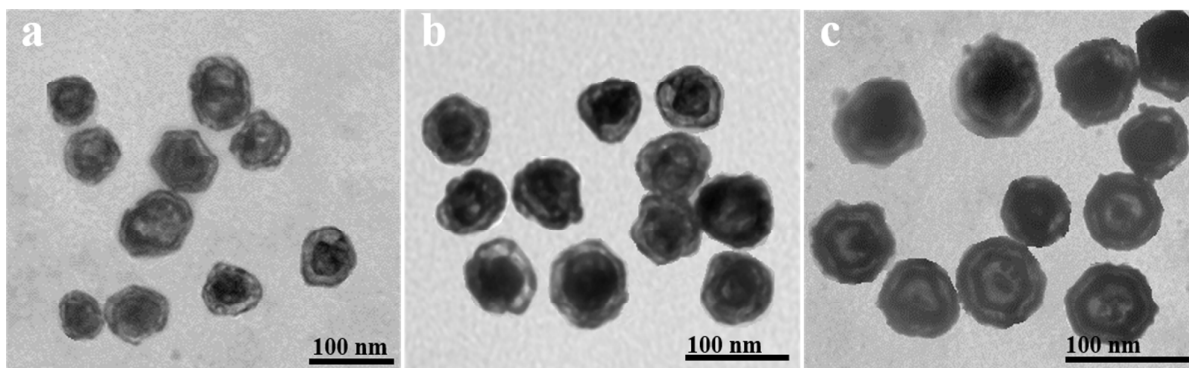


Figure S2. TEM images of IONP@shell-in-shell with various amounts of HAuCl₄ in feed (a) 1.0 μmol, (b) 1.5 μmol and (c) 2.0 μmol.

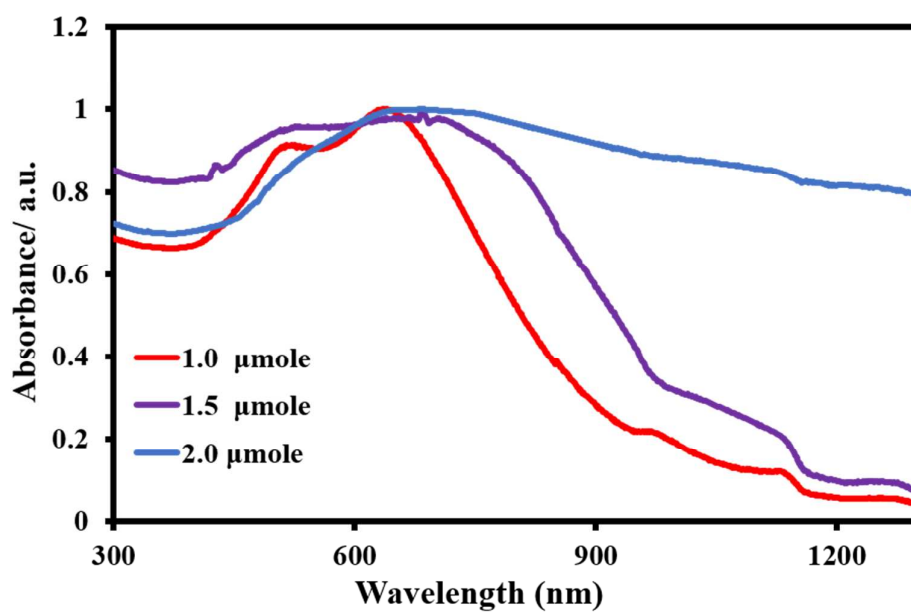


Figure S3. (a) UV-vis-NIR spectra of IONP@shell-in-shell synthesized using various amounts of HAuCl₄ in feed.

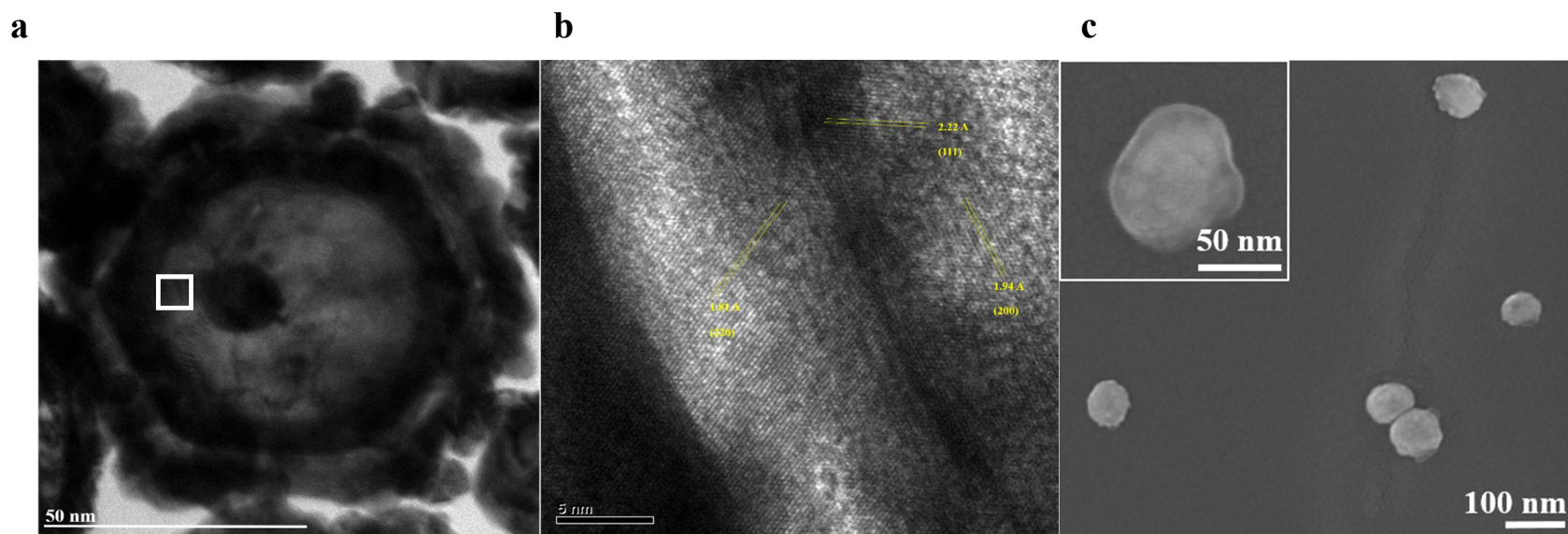
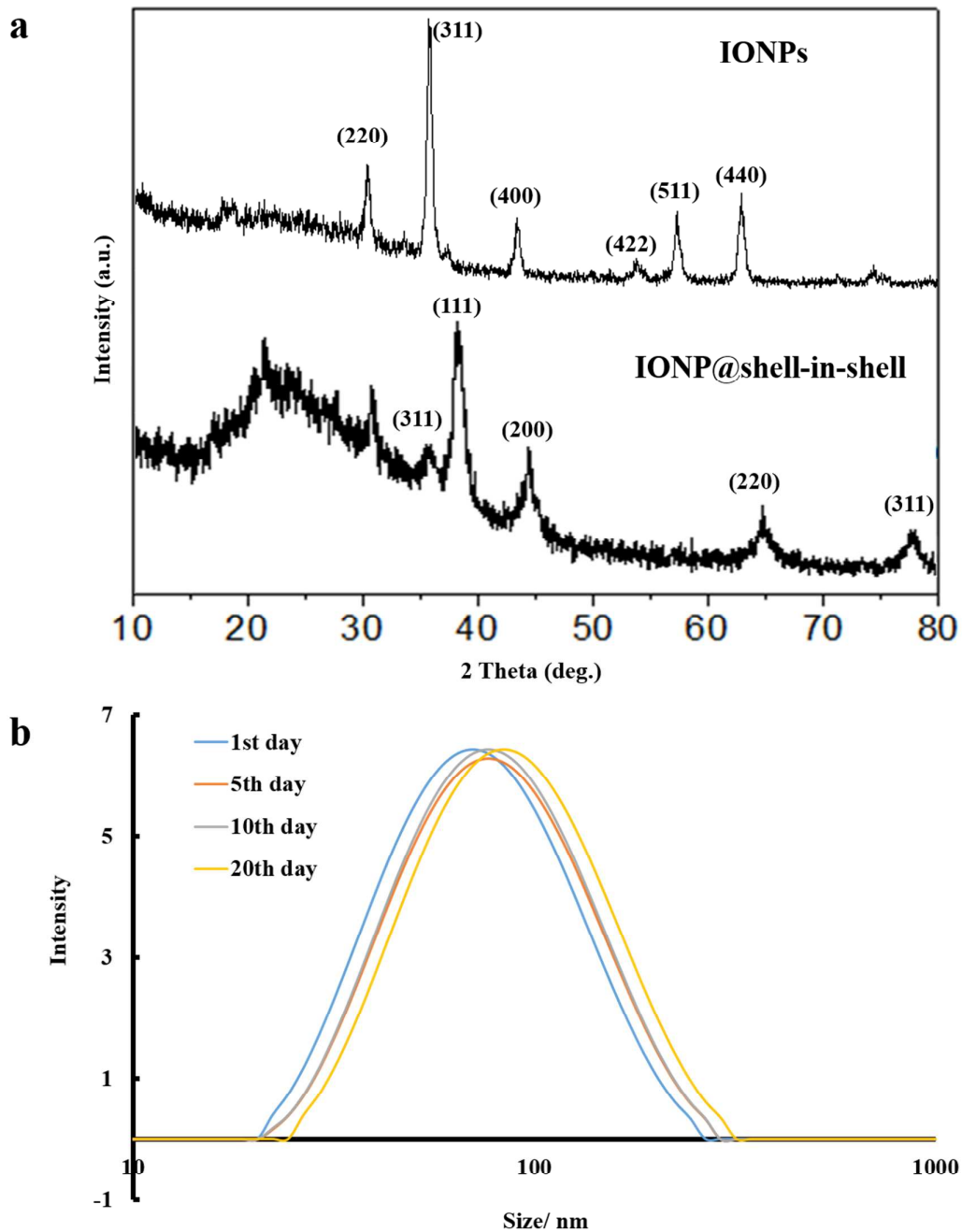


Figure S4. (a) The HR-TEM image of a single IONP@shell-in-shell NP and (b) the magnified image of the marked white square in (a) to estimate the lattice distance of the IONP@shell-in-shell NPs. (c) The HR-FESEM image of the IONP@shell-in-shell NPs to observe the surface morphology and the outer shell.



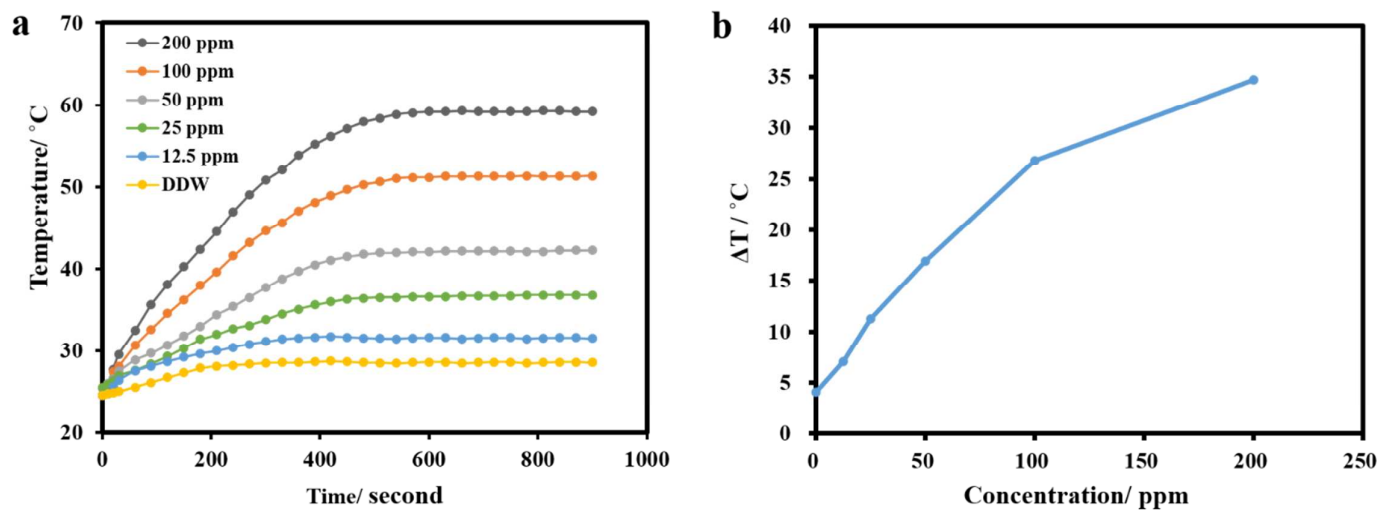


Figure S6. (a) Photothermal heating curves of double deionized (DD) water and IONP@shell-in-shell in DD water (12.5, 25, 50, 100, and 200 ppm of Au ion) as a function of irradiation time using a 1064 nm diode laser (0 -15 min). (b) A plot of temperature change ΔT (the temperature at 15 min minus the room temperature of 24.5 °C, $T_{15\text{min}} - T_{\text{RT}}$) versus concentration.

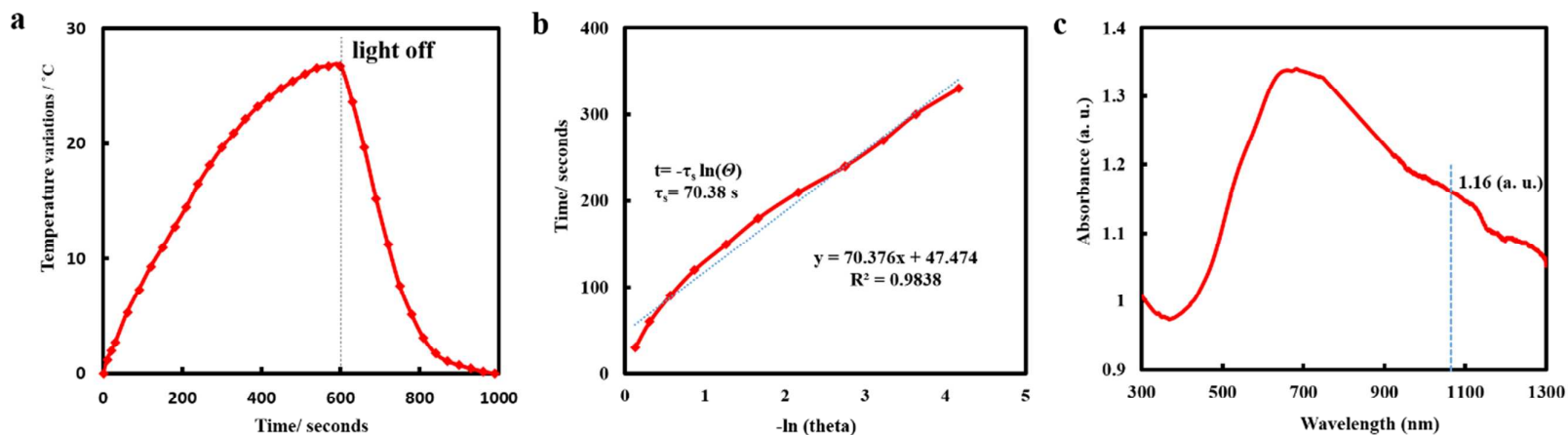


Figure S7. (a) Temperature change of IONP@shell-in-shell at an Au ion concentration of 100 ppm upon 1064 nm diode laser irradiation (3 W cm^{-2}) for 10 min, followed by turning it off. (b) A linear plot of time (after 600 s) versus negative natural logarithm of dimensionless driving force temperature obtained from the cooling stage of curve (a) to calculate the time constant for heat transfer from the system. (c) UV-vis-NIR absorption spectrum of IONP@shell-in-shell at an Au ion concentration at 100 ppm. A blue dash line is absorbance value at 1064 nm.

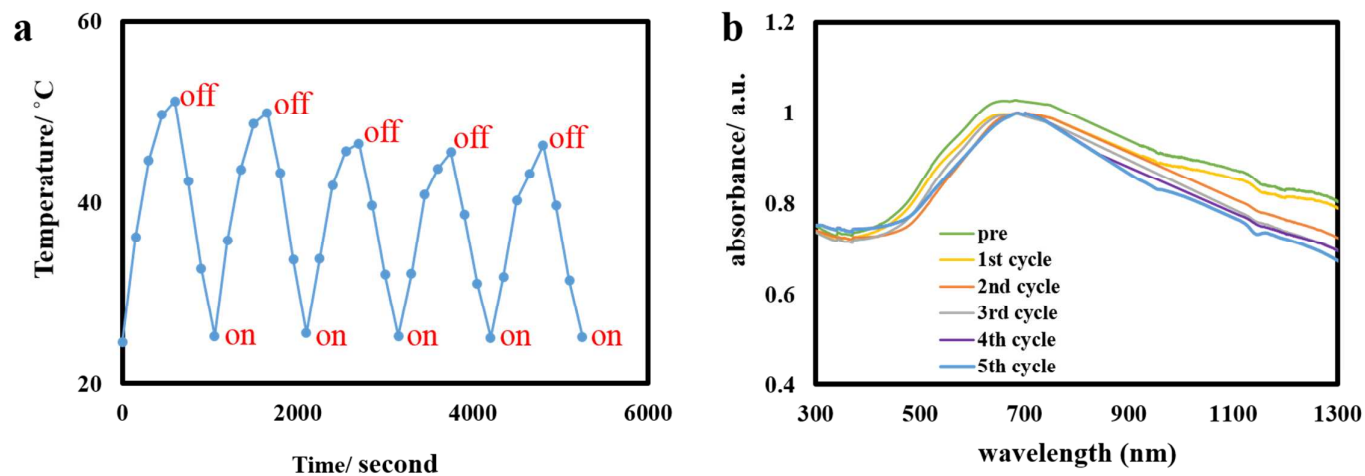


Figure S8. (a) Real-time thermal response curves and (b) UV-vis-NIR spectra of IONP@shell-in-shell at an Au ion concentration of 100 ppm in aqueous dispersion upon 1064 nm diode laser irradiation (3 W cm^{-2}) for 10 min, followed by turning it off for 7.5 min during five cycles for testing photostability.

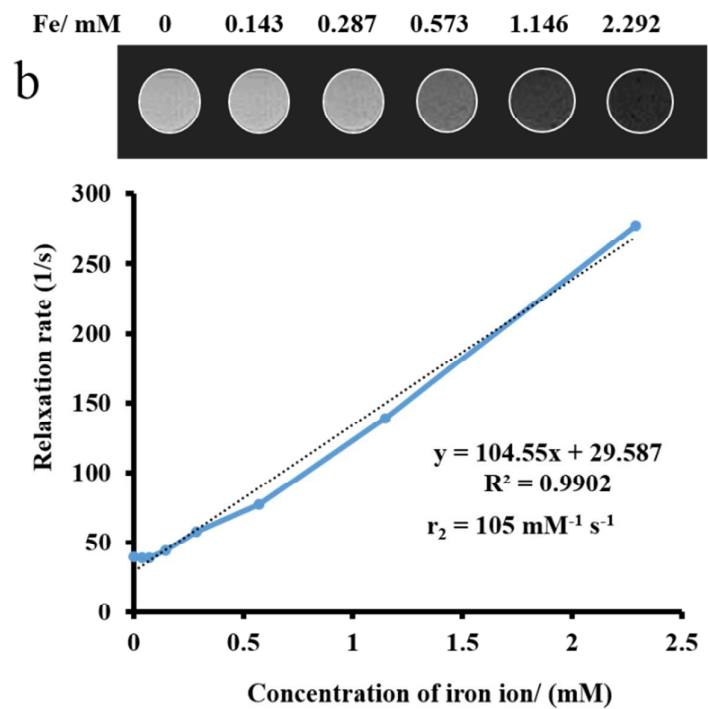
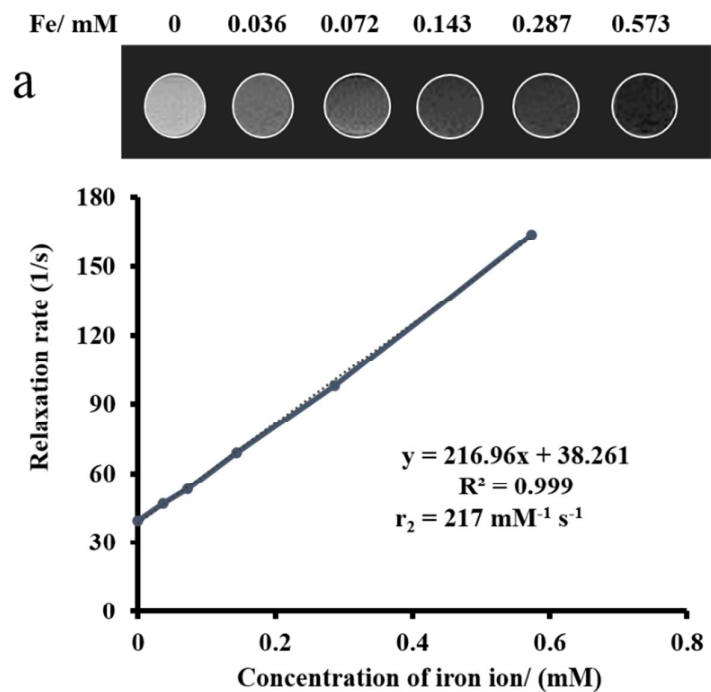


Figure S9. Relaxivity r_2 values of (a) IONPs and (b) IONP@shell-in-shell calculated from T_2 relaxation (T_2^{-1}/s^{-1}) rate versus Fe ion concentration.

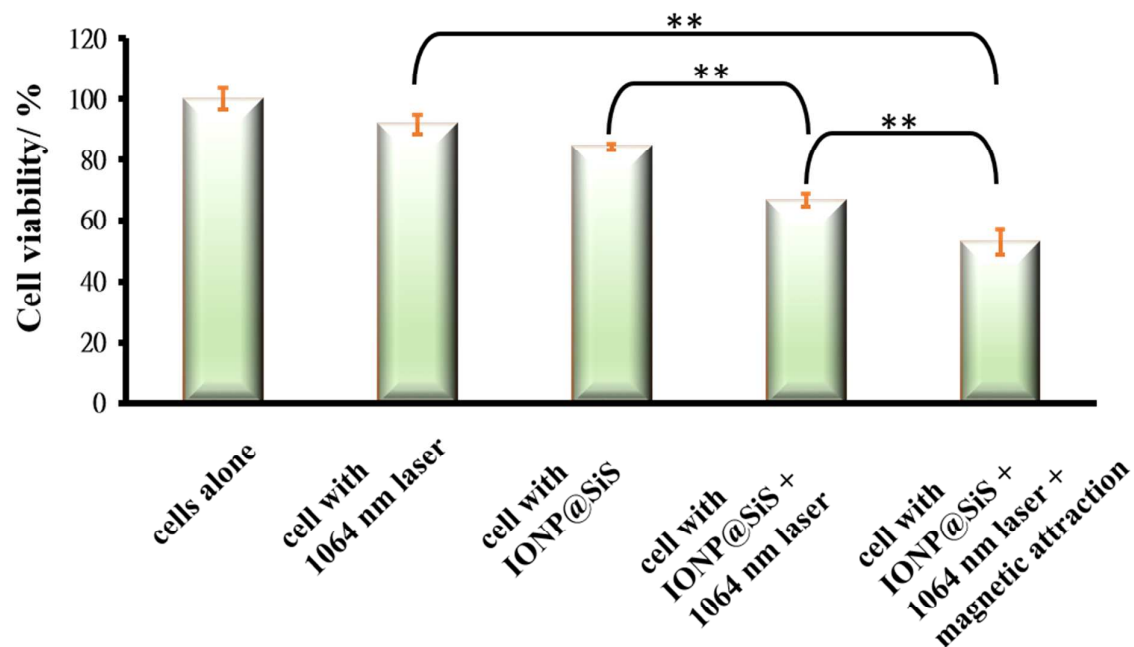


Figure S10. Cell viabilities of U87 cells exposed to IONP@shell-in-shell at an Au ion concentration of 100 ppm and with indicated treatments and analyzed by MTT assay. The cells were treated underneath MagnetoFACTOR-96 plate for 1.5 h, followed by irradiation with a diode laser of power density 3 W cm^{-2} for 10 min ($n=8$, $**p < 0.01$).

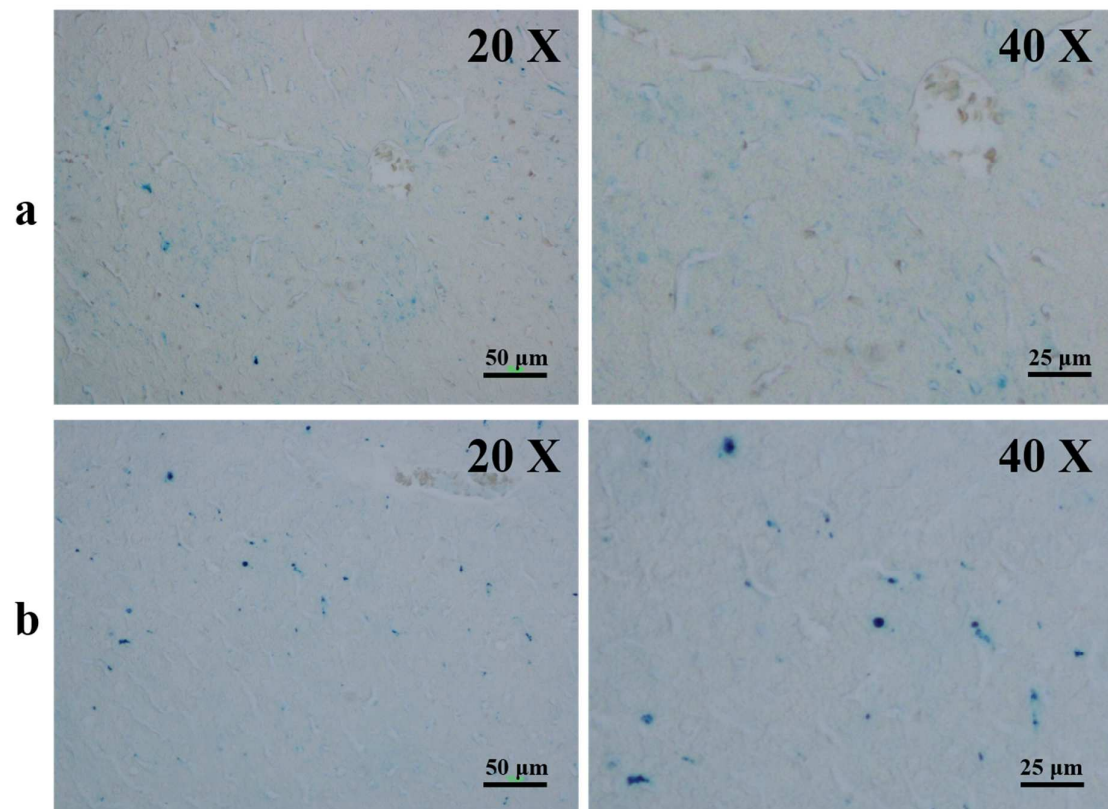


Figure S11. Micrographs of the brain tumor stained by Prussian blue (a) without and (b) with magnetic assistance. IONP@shell-in-shell NPs in PBS were administered to the mouse via a tail vein injection at a dosage of 20 mg kg^{-1} with or without an external magnetic field for 30 min. The tumor tissue was dissected from the mouse at 24 h post-injection.

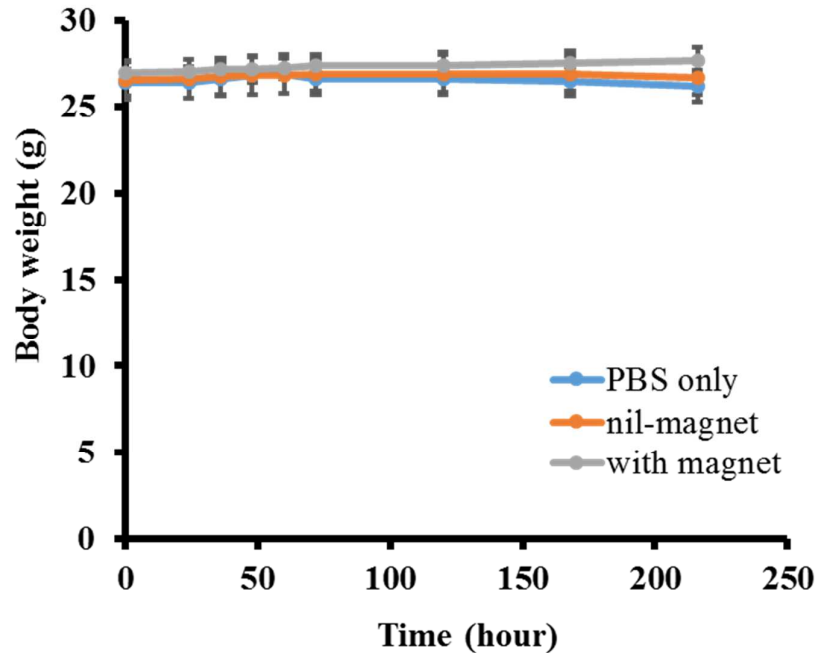


Figure S12. Body weights of mice measured pre-injection (pre) and post-injection at 24, 36, 48, 60, 72, 120, 168 and 216 hours, respectively. Mice were administered with PBS (blue color), and with IONP@shell-in-shell NPs (b, c) in PBS via the tail vein at a dosage of 20 mg kg^{-1} (b) without (orange color) and (c) with (gray color) magnetic assistance. The magnet was applied near the tumor site for 30 min after injection of NPs and the tumor region was irradiated with a 3 W cm^{-2} 1064 nm diode laser for 20 min ($n=4$).